Project Team 12
Spontaneous magnetization- induced phonons stability in γ'-Fe_4N crystalline alloys and high-pressure new phase

Antonio Vázquez López* and Jaime Dolado Fernández†
Department of Materials Physics,
Complutense University of Madrid (UCM)

(Dated: December 2020)

Herein, we show our project results, which is based on the calculations performed by Cheng et al. [1] studying magnetic γ'-Fe_4N crystalline alloy by density-functional theory. This alloy presents a new phase induced at high pressures found out by the presence of soft phonon modes. Spontaneous magnetization at pressures near 1 GPa are also observed. At 10 GPa a new phase appears with symmetry group P2/m. Herein we tried to unravel this effects by studying the lattice distortions and atomic positions with DFT relaxation calculations, assessing the values of the magnetic moment on the different atoms and the most stable configurations.

I. INTRODUCTION

γ'-Fe_4N possesses cubic structure where the nitrogen atoms are into octahedral interstitial positions. Its space group is $Pm\bar{3}m$. The structure can be observed in FIG.1. This material has been studied mainly because its simplicity and magnetic properties, in particular interest as a catalyst for amonia production or as a high-density magnetic recording device [2]. In this paper, authors affirm that the softening at the M point at 10 GPa evolves into a new phase of P2/m Fe_4N, which opens a study on a new phase for this material.

II. METHODS

The DFT calculations in this paper were performed with the QUANTUM ESPRESSO code [3] and the PBE exchange-correlation functional. Pseudopotentials chosen taking into account the recommendations on the article, the exchange interaction between electrons adopts Perdew-Burke-Ernzerhof (PBE) The projector augmented wave (PAW) method is used to calculate the electron-core interactions. The relaxation of atoms adopts first-order Methfessel-Paxton smearing method. Calculations are spin-polarized, so correct .UPF were chosen and an starting magnetization was selected to each atom.

Firstly, convergence test were executed (see Appendix V) where different parameters are evaluated until sufficient precision in the calculation is achieved in reasonable amount of time, considering limited computing resources. As an of the parameters to be determined are the *k-mesh* (number of k-points on the First Brillouin zone, *ecutrho* and *ecutwf* which determine the basis set size for the wavefunction and, respectively. Following recommendations on the chosen pseudopotentials, a ratio *ecutrho*/*ecutwf* of 7 was initially evaluated. After convergence testing *ecutrho* and *ecutwf* were set to 1050 and 150 Ry, respectively with a *k-mesh* of 7x7x7. Values of the intial .cif file were obtained from [4]. In FIG.1 γ'-Fe_4N is represented the value of a selected initially was 3.673673 Å. The initial values of the cell parameters were under estimated in comparison with the used on the article. With this lattice parameters the convergence testings were calculated. In section III A value was corrected to the same that in [1], 3.79500, and the cell optimization was performed. Similar values on the single magnetic moment on each atom was found, showing negative magnetic moment induced on the N atoms.

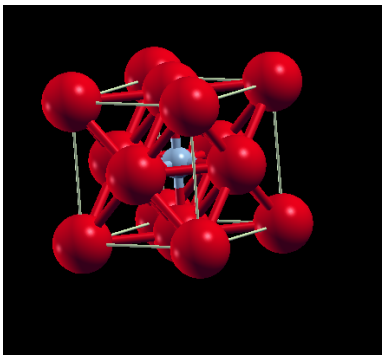

FIG. 1. Primitive cell for γ'-Fe_4N where Fe is represented in red color and N in grey.

III. DFT RESULTS

A. Geometrical optimization

After determining the initial parameters, a full optimization (cell volume and atoms positions) was performed.

* antvaz01@ucm.es
† jdolado@ucm.es

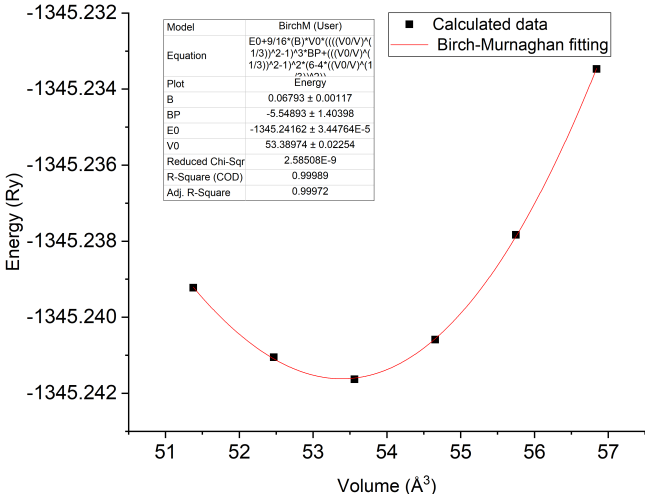

FIG. 2. E-V plot of the γ'-Fe_4N structure

In FIG.2 shows the E-V plot of the calculated energies for different volumes. From the table inset in the graph we observe that the optimal volume as predicted by the Birch-Murnaghan equation is ∼53.30-53.38 Å^3, depending on the calculation procedure (with OriginPro fitting to the equation or using the ev.x tool of QE). With this new volume, we optimize positions of the atoms on the cell via a *vc-relax* calculation with target pressures of 10, 30 and 40 GPa.

P_o (GPa)	P_f (GPa)	V_f (Å^3)	$\frac{a}{c}$ -	E (Ry)	Total M (μ_B/cell)
10	10.09	50.12873	0.97976	-1345.23514218	4.77
30	30.005	45.36030	0.94765	-1345.19408068	0.92
40	40.003	44.17000	0.9392	-1345.17599489	0

TABLE I. Obtained hydrostatic pressure, Energy and total magnetization after full optimization using vc-relax

Table I shows that the total magnetization decreases with increasing target pressure and goes to 0 at 40 GPa. This is in accordance with the article, as in the conclusion is stated that below 40 GPa the magnetic moment of the Fe1 atoms decrease with increasing pressure and collapse at 40 GPa.

B. M instability

At 10 GPa there is an imaginary frequency at the M point, which is usually called soft mode. This is a clear indicator that the structure is not stable. As determined in the article, a .cif file is constructed. The angle is not determined by authors so for a monoclinic-type structure an initial angle of 110° seems reasonable. The structure can be observed on FIG.3.

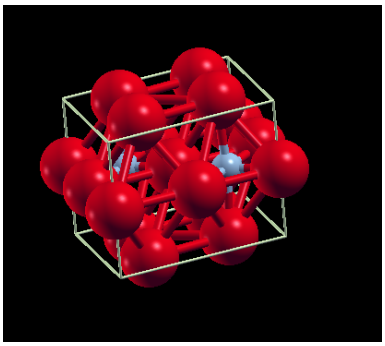

FIG. 3. Primitive cell for γ'-Fe_4N as P2/m after 10GPa

ISODISTORT [5] allows us to understand which structure could be more stable.
`M5- C1 (0,0;a,b;0,0) 10 P2/m, basis=(1,0,1),(0,1,0),(-1,0,1), origin=(0,0,1/2), s=2, i=24, k-active= (1/2,0,1/2)` Fits what is stated on the article.

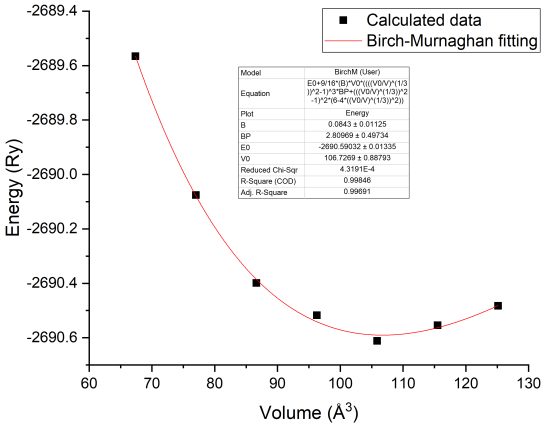

FIG. 4. E-V plot of the γ'-Fe_4N structure at 10 GPa, P2/m.

FIG.4 shows the calculation of the bulk modulus for this new phase. It must be pointed out that for some reason those calculations employ much more computational time and many of the calculations stopped due to high demand on memory. For that, in this case the *ecutrho*/*ecutwf* was stick to 7 but respectively values were lowered to 700 and 100 Ry, and the mesh used 1x1x1 which is really small for quality calculations.

C. X instability

Similarly, at 30 GPa a soft mode is observed, in this case at the X-point. In this case there is no specification of which phase is induced. Using the same tool as before, the possibilities were listed on the video. Orthorrombic system appears the most. For that, for us seem

reasonable to think that this is the Bravais lattice that the system adopts at high pressure, the difference with the previous phase is that now the angles will be equal to 90° while the cell parameters remain different.
For absence of time, the procedure will be the same than for the two previous parts, construct a .cif file for the space group with Wyckoff symbol of 51 or 63 and run the calculations.

```
  X5- P1 (a,-a;0,0;0,0) 63 Cmcm,
basis=(1,0,1),(1,0,-1),(0,2,0),
origin=(0,1/2,0), s=2, i=12, k-active=
(0,1/2,0) ORTHORROMBIC
  X5+ P2 (0,a;0,0;0,0) 51 Pmma,
basis=(0,2,0),(-1,0,0),(0,0,1),
origin=(0,0,0), s=2, i=12, k-active= (0,1/2,0)
ORTHORROMBIC
```

D. Miscellaneous

In section III before obtaining the bulk modulus for the case of the Pm$\bar{3}$m structure, a lot of calculations were done underestimating the cell parameters (not shown here). From that, the relation of the Total magnetic moment and the pressure was obtained and follows a similar path that shown in Table I and is show in the FIG.5 below. It is observed that the magnetic moment abruptly goes to 0 at 20-40 GPa, what is in agreement with the results of the article.

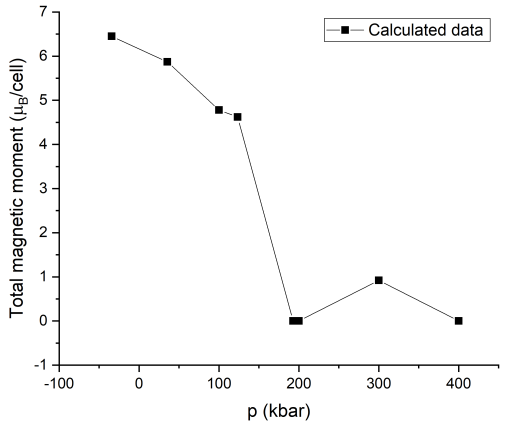

FIG. 5. Pressure and Magnetization

IV. CONCLUSIONS

In summary, we amied to replicate some of the calculations shown on the article by Cheng et al. [1]. After initial determination of the proper convergence values, a full cell optimization on the Pm$\bar{3}$m structure was performed and the bulk modulus was obtained, showing that the lattice tends to a subtle compression stability. The presence of soft modes in 10 GPa shows that spontaneous magnetization and pressure induces a phase change on the structure to a P2/m structure for which, an initial optimization of the cell parameters was only obtained. At 30 GPa the there is also presence of soft modes, from the information found in ISODISTORT the different candidates of the new cell structure were addressed. Lack of time and long computational calculations left part of the work undone such as the use of PHONOPY and the calculation of the dispersion bands for phonons. Even though, convergence and optimisation of the γ'-Fe_4N , its magnetic properties and dependence with pressure were addressed.

ACKNOWLEDGMENTS

We wish to acknowledge our colleague Y. Baba for allowing us to run most of the calculations on her computer. We would like also to thank Dr. S. Cottenier for such a magnificent course and its support throughout.

V. APPENDIXES

TABLE II. Hydrostatic pressure as a function of the k-mesh, with *ecutrho*=50 *ecutwfc*=500

k-mesh	Pressure (kbar)	Time (s)
1x1x1	75.81	1m31.96s
2x2x 2	-214.14	1m44.29s
3x3x3	-182.00	1m46.44
4x4x4	-195.32	2m25.49s
5x5x5	-197.51	2m51.00s
6x6x6	-193.71	4m22.75s
7x7x7	-193.83	4m14.63s
8x8x8	-194.42	6m29.00s
9x9x9	-194.74	6m52.33s
10x10x10	-194.43	10m45.40s
11x11x11	-193.56	11m 2.45s
12x12x12	-194.34	15m54.49s
13x13x13	-194.78	17m 4.79s

TABLE III. Hydrostatic pressure as a function of the *k-mesh*, with *ecutrho*=200 and *ecutwfc*=50

k-mesh	Pressure (kbar)	Time (s)
1x1x1	79.24	1m24.98s
3x3x3	-178.07	2m9.79s
5x5x5	-192.94	2m52.87s
6x5x5	-191.06	5m22.91s
7x7x7	-189.87	5m21.62s
8x8x8	-189.67	7m56.25s

TABLE IV. Hydrostatic pressure as a function of the *k-mesh*, with *ecutrho*=200 and *ecutwfc*=50 setting *smearing=mv*

k-mesh	Pressure (kbar)	Time (s)
1x1x1	221.78	5m49.03s
2x2x2	-90.75	9m25.27s
5x5x5	-83.26	16m56.09
6x6x6	-66.80	29m39.62s
7x7x7	-60.99	21m37.14s
8x8x8	-57.20	34m55.08s
9x9x9	-63.37	37m39.51s
10x10x10	-57.76	48m59.23s
11x11x11	-59.64	50m59.27s
12x12x12	-60.45	1h14m

TABLE V. Hydrostatic pressure as a function of the *k-mesh*, with *ecutrho*=200 and *ecutwfc*=50 setting *nspin=2*

ecutrho /*ecutwfc* ratio	*ecutwfc*	*ecutrho*	Pressure (kbar)	Time(s)
5	100	500	-9.58	15m14.53s
6	100	600	-9.62	14m47.34s
7	100	700	-9.55	15m 2.67s
8	100	800	-9.62	15m34.39s

TABLE VI. Hydrostatic pressure as a function of *ecutrho*/ *ecutwfc* ratio for *k-mesh* 7 x 7 x 7

ecutwfc	*ecutrho*	Pressure (kbar)	Time(s)
10	70	-60072.75	1m19.08s
20	140	-68113.48	2m 0.29s
30	210	-68113.48	1m55.90s
40	280	-2538.38	4m18.52s
50	350	-213.03	4m35.86s
60	420	-25.89	7m37.78s
70	490	-51.81	10m22.48s
80	560	-39.08	11m14.27s
90	630	-16.75	13m38.52s
100	700	-9.55	15m49.62s
110	770	-12.04	16m44.58s
120	840	-13.93	19m 4.67s
130	910	-12.81	22m55.56s
140	980	-10.52	24m45.70s
150	1050	-9.22	29m28.46s
160	1120	-9.26	34m32.81s
170	1190	-9.94	31m 2.88s
180	1260	-10.13	33m11.39s
190	1330	-9.99	34m 3.87s
200	1400	-9.60	37m40.98s

TABLE VII. Hydrostatic pressure as a function of *ecutwfc*for *k-mesh* 7 x 7 x 7 while *ecutrho*/ *ecutwfc* ratio is kept constant at 7 and the *ecutwfc* is varying.

[1] Y. S. L. Z. L. L. Tai-min Cheng, Guo-liang Yu, Journal of Magnetism and Magnetic Materials **451**, 87 (2018).

[2] N. E. C. H. E. Eitel L. Peltzer y Blancá, Judith Desimoni and S. Cottenier, Phys. Status Solidi B **5**, 909–928 (2009).

[3] Quantum espresso, `https://www.quantum-espresso.org/`.

[4] materials project, `https://materialsproject.org/materials/mp-535/`.

[5] Isodistort, `https://stokes.byu.edu/iso/isodistort.php`.